

## COMPARISON OF TWO TRANSPORT DESCRIPTORS WITHIN A HYBRID RECEPTOR MODELING SYSTEM

John M. Shuford<sup>1</sup>, John G. Eoll, Stephanie L. Seely, William G. Moore & Joseph G. Dreher  
ENSCO Inc., Melbourne, FL

### 1. INTRODUCTION

ENSCO, Inc. is developing systems for imputing source locations using transport and dispersion modeling in combination with sample records of pollutant concentrations. These data are analyzed within the general framework commonly referred to as hybrid receptor modeling in which a statistic (an estimate of conditional probability) is calculated for each grid square based on the relative strength of association between the passage of air parcels over that grid square and the arrivals of those air parcels at the receptor during times of elevated pollutant concentrations.

Conditional probability surfaces can be estimated using both forward and backward descriptors of transport. In both approaches, we use a statistical bootstrapping algorithm to obtain confidence intervals on the conditional probability estimates. In the forward-transport approach, the conditional probability field is estimated from simulated airborne concentrations at a receptor arising from hypothetical plumes arriving from each point of a grid of hypothetical sources. The simulated airborne concentrations are produced by the transport and dispersion model SLAM (Kienzle 1989), which is a Lagrangian Gaussian-puff and trajectory model that can ingest a wide variety of meteorological data and formats. In the backward modeling approach, the conditional probabilities are estimated from frequency counts of backward-trajectory segment endpoints in the various cells of the grid. When used with backwards trajectories, it is similar to Hopke's PSCF model used with bootstrapping (Hopke et al., 1995).

We have used the new model in both modes to analyze airborne concentration and trajectory data over the Southwestern United States using data from a project which investigated sources of haze in Grand Canyon National Park during the mid-to-late 1980's. Our results are compared and contrasted with previously published results.

### 2. BACKGROUND

As a convenient and interesting test case for observing and comparing the results obtained using backward- and forward-trajectory frameworks for hybrid receptor modeling, we have chosen to analyze data from

the Subregional Cooperative, Electrical Industry, Department of Defense, National Park Service and EPA Study (SCENES) on visibility around the Grand Canyon. That study was conducted during a period spanning 1983 to 1989. One of several objectives of the SCENES study was to identify potential pollution sources in the U.S. Southwest that might be contributing significantly to haze levels at Grand Canyon National Park.

We have not attempted to perform a comprehensive analysis of the data from SCENES; rather, we have focused merely on applying hybrid receptor models to a set of PM<sub>2.5</sub> measurements of air filtration samples collected at Hopi Point, Arizona, an observation point located on the South Rim of the Grand Canyon (36°04'N-112°09'W, 2,150 MSL). Thorough analyses of these data have been previously published (Vasconcelos, Macias, & White, 1994; Vasconcelos, Kahl, Liu, Macias, & White, 1996; Vasconcelos, 1999) and we refer the reader to those references for more detailed description of the experimental protocols and data. Indeed, a significant factor in our decision to analyze these data was the fact that the Vasconcelos, *et al* papers provided an authoritative baseline to which we could compare our results.

### 3. MATERIALS AND METHODS

#### 3.1. Transport Descriptors and Adopted Grid

The original study, summarized by Vasconcelos (1999), used the Air Resources Laboratories Atmospheric Transport and Dispersion (ARL-ATAD) model to estimate 72-h back trajectories arriving at the Hopi Point, Arizona receptor site. Input to the ARL-ATAD model consisted of National Weather Service and U. S. Air Force rawinsonde observations data to produce the 72-h backwards trajectories. Our analysis used the Trajectory CALCulation (TCAL) model, which is a single-layer, Gaussian puff transport-dispersion model. Where ATAD determined the depth of the transport layer using temperature and pressure profiles at rawinsonde stations within 560 km., TCAL used two predefined mixed layer depths for nighttime and daytime transport (500 m and 1500 m, respectively). Input to TCAL consisted of archived hourly surface and twice daily rawinsonde observations. Unlike Vasconcelos (1999), we did not have any access to special surface and/or rawinsonde observations surrounding GCNP; however, global gridded NCEP/NCAR reanalysis fields were used as input to

---

1. Corresponding author address: 4849 N Wickham Rd., Melbourne, FL 32940. email: shuford.john@ensco.com.

TCAL ( $2.5^\circ \times 2.5^\circ$ ; Kalnay et al. 1996). Simulations were performed for the period July 1984 to September 1989. Both TCAL and ARL-ATAD calculate two-dimensional advection using horizontal winds averaged throughout the mixed layer to obtain the estimated position of an air parcel at regular intervals (hourly for TCAL, 3-hourly for ATAD) throughout the 72 hours until its arrival at a receptor location. We did not attempt to exclude backwards trajectories that ended prematurely because of missing data, or those that contained endpoints outside the study domain.

To produce the forward descriptor of transport, we used the Short-range Layered Atmospheric Model (SLAM) which used the same archived surface observations, rawinsonde data, and global gridded NCEP/NCAR reanalysis fields that were used as input to TCAL. SLAM is a multiple layer, Gaussian puff, transport-dispersion model. Within the model, continuous or intermittent releases of gases or particulates are simulated by the release of large numbers of puffs, which grow and advect downwind based on the mean wind within the transport layer. The mean transport layer is adjusted based on spatially and temporally changing patterns of the planetary boundary layer height (PBL). As the mixing depth changes along the path of a puff, the puff may split into multiple vertical levels, with each partition utilizing its unique transport layer winds. SLAM can model the transport of material based on a wide array of meteorological wind datasets, including conventional surface and upper air observations, global 2.5-, 1-, and 0.5-degree gridded analyses and forecasts, as well as output from the Regional Atmospheric Modeling System (RAMS; Pielke et al. 1992) and the fifth Generation Mesoscale Model (MM5; Grell et al. 1994). Based on the puffs' advection, dispersion, and vertical extent, SLAM calculates hourly concentration estimates at user-selected locations at the ground and aloft. Mass losses due to dry and wet deposition as well as environmental decay can also be modeled; however, we did not utilize those options for this study.

SLAM was configured to model puffs emitted at intervals of 60 minutes from a grid of 391 sources covering the western half of the United States. A depiction of the grid along with the location of surface and rawinsonde observations used as input to SLAM is shown in Figure 1. Wind vectors to determine transport were recalculated every 60 minutes and puffs were tracked for 72 hours. In order to speed model execution, simulations did not take into account winds above 2500 meters AGL, and higher mixing heights were capped to that level.

### 3.2. SAMPLER DATA

Aerosol fines data for the Grand Canyon were obtained from the Center for Air Pollution Impact and Trend Analysis (CAPITA), School of Engineering, Washington University (SCENES Data). That data set consists

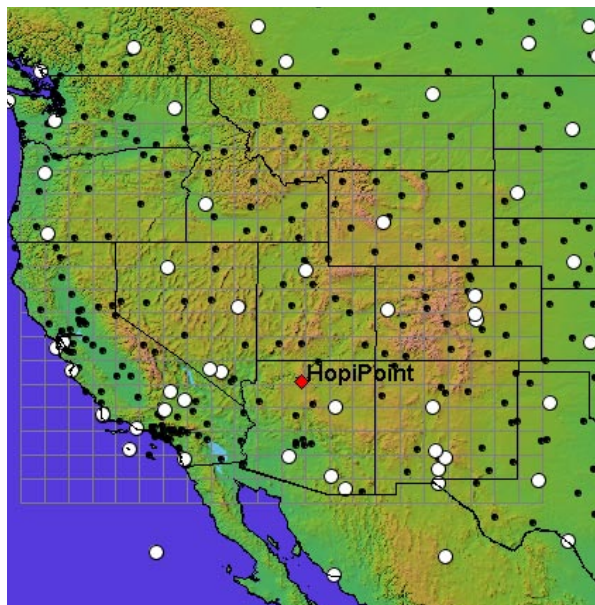


**Figure 1. Locations of the surface (black dots) and rawinsonde (white circles) sites used as input to the SLAM gridded source simulations and TCAL. Receptor location at Hopi Point is represented by the red diamond.**

of daily gravimetric mass measurements of PM<sub>2.5</sub> taken from May, 1984 to September, 1989. For convenience, we used a subset of this data: July, 1984 to April, 1988. The seasonal variation of aerosol mass data is shown in Figure 2.

These data were collected by an automated sampler located at Hopi Point and operated by Desert Research Institute for the SCENES program. Collection time occurred at 1900 local time (Mountain Standard Time, MST), and was presumed to be 24 hours in length, terminating at the time of collection (Vasconcelos, Macias & White, 1994).

### 3.3. BACKWARD TRAJECTORY FRAMEWORK: PSCF AND CWT

The Potential Source Contribution Function (PSCF) model is a widely used hybrid receptor model used for inferring potential source locations. The PSCF approach was originally developed by Ashbaugh *et al.* (1985), and Malm *et al.* (1986). It calculates conditional probabilities associated with a geospatial grid which is overlaid onto the region of interest. The grid must be large enough to encompass suspected or known sources of the material of interest as well as the single receptor location. The calculation of PSCF factors is actually quite simple in practice. If  $n_{ij}$  trajectory segment endpoint falls onto the  $ij$ -th cell, the probability of this event  $A_{ij}$  is given by:

$$P[A_{ij}] = n_{ij} / N, \quad (1)$$

where  $N$  is the total number of segment endpoints summarized over all cells in the calculational grid.

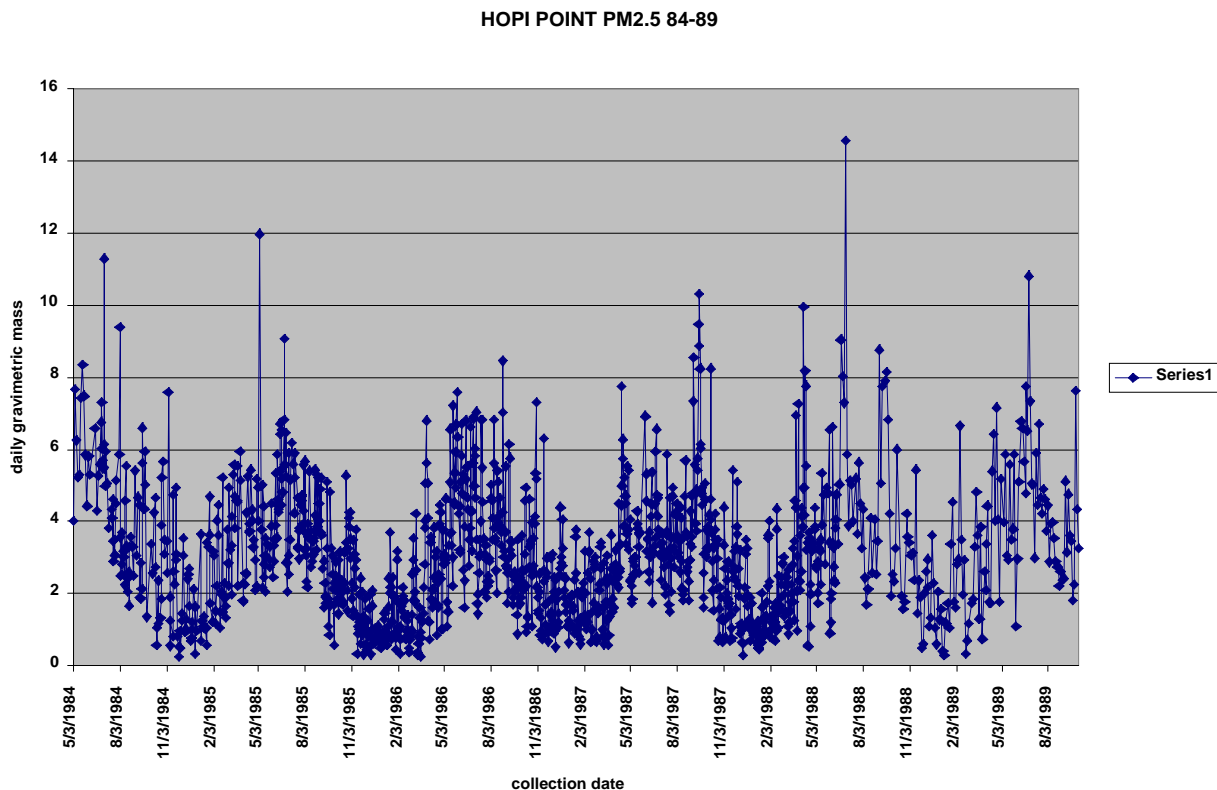


**Figure 2. Measured quantity of PM<sub>2.5</sub> in samples collected at Hopi Point from May 1984 to August 1989.**

In the same  $ij$ -th cell, if there are  $m_{ij}$  endpoints that correspond to all the trajectories that ended at the receptor site during sampling periods with pollutant concentrations higher than some pre-specified (presumably significant) amount, then the probability of this event  $B_{ij}$  is:

$$P[B_{ij}] = m_{ij} / N \quad (2)$$

The potential source contribution function (PSCF) is then defined as a conditional probability:

$$PSCF_{ij} = P[B_{ij}] / P[A_{ij}], \quad (3)$$

which is equal to the ratio  $m_{ij} / n_{ij}$ .

The  $PSCF_{ij}$  is then the conditional probability that an air mass with specified material of interest concentrations arrived at the receptor site after having passed through (resided in) the  $ij$ -th cell. Cells for which high PSCF values are calculated are the "potential" source areas.

A version of the Potential Source Contribution Function (PSCF) model was obtained from P. Hopke of Clarkson University and coded into FORTRAN. We used it to map potential sources for airborne aerosols consisting of particulate matter < 2.5 microns, PM<sub>2.5</sub> (for a review of the PSCF method, see Begum *et al.*, 2005).

PSCF factors were then calculated for each of the four seasons, 1985 through 1988, where the seasons are defined according to the convention followed by Vasconcelos (1999). Under this convention, the summer season is defined as consisting of the months June, July, and August. One implication of that choice is that a well known climatological shift (the "Arizona Monsoon") which usually occurs in early July falls within season rather than between seasons. That shift is the transition into the southeastern monsoonal flow from the gulf of Mexico. According to National Weather Service, the average date of the onset of the monsoon is July 7 (NWS -- *The Arizona Monsoon*). As a result, we might expect the PSCF results for Summer to suffer some increased ambiguity (i.e. a more widespread, ill-defined source region) due to this climatic effect.

#### **3.4. FORWARD TRAJECTORY FRAMEWORK: GFTR**

In the forward-transport approach, the conditional probability field is estimated from predicted "catch" of airborne particulates at a receptor collected from hypothetical plumes originating from each point of a grid of putative sources. In our case, the predicted airborne concentrations are calculated by the transport and dispersion model SLAM, which is a Lagrangian Gaussian-

puff and trajectory model that can ingest a wide variety of meteorological data and formats.

To sharpen these ideas, we will specify more explicitly what is meant by the predicted “catch” from a grid-point source. To this end, suppose aerosol “puffs” of unit mass emanate at regularly spaced time intervals comprising the set  $R = \{r_k \mid k=1,2,\dots,K\}$  from a hypothetical source at grid coordinates  $(i, j)$ . Let

$$\kappa_{i,j,r_k}(x,t) \quad (4)$$

denote the predicted effluent concentration at receptor location  $x$  at time  $t$  due to the unit-mass puff released at (earlier) time  $r_k$  from grid-point source  $(i, j)$ . Then, if  $\varphi(t)$  denotes the throughput of the sampler ( $\text{m}^3/\text{hr}$ ) during sampling period  $S=[a, b]$ , then

$$C_{i,j}(x,S) = \int_a^b \left[ \sum_{r \in R} \kappa_{i,j,r_k}(x,t) \right] \varphi(t) dt \quad (5)$$

represents the predicted “catch” by a sampler at location  $x$  during sampling period  $S$  from the hypothetical releases at grid-point  $(i, j)$ .

For each candidate grid-point source, we seek to devise a statistic that estimates the likelihood that transport of material from that source will result in “interesting” samples. An “interesting” sample is one in which we detect the effluent of interest in some reliable, reproducible way and for which we assess the concentration to be elevated with respect to ambient background levels. Our general strategy then would be to devise methods that will highlight sources that have higher than expected values of the statistic or that are correlated with “interesting” samples to a degree not adequately explained by random chance and mere climatology.

To that end, we define the Grid-point Forward Transport Ratio (GFTR) for each grid-point. For a given sampling campaign at a given receptor location, GFTR is, notionally, the total estimated catch during “interesting” samples divided by the total estimated catch during all samples. More specifically, let

$$S = \{s_n = [a_n, b_n] \mid n = 1, 2, \dots, N\} \quad (6)$$

denote a succession of sampling periods at the subject receptor location  $x$ , and let  $C_{i,j}(x, s_n)$  denote the predicted “catch” by a sampler at location  $x$  during sampling period  $s_n$  due to “steady continuous” unit releases from a hypothetical source at grid point  $(i, j)$ . If we let

$$I(n) = \begin{cases} 1, & \text{if } s_n \text{ is an interesting sample} \\ 0, & \text{otherwise} \end{cases}, \quad (7)$$

we can then define

$$GFTR(i, j | x, S) = \frac{\sum_{n=1}^N [C_{i,j}(x, s_n) \cdot I(n)]}{\sum_{n=1}^N C_{i,j}(x, s_n)}. \quad (8)$$

For some grid cells, the raw GFTR values may be supported by a relatively small number of samples; i.e., it is possible to calculate a GFTR score for a given grid cell when only one or a few samples register nonzero “catch” from that grid cell. If all or most of those samples are “interesting” according to the pre-selected threshold, that GFTR value may be quite high -- even unity -- despite the fact that the putative “source” at that grid cell “explains” only a small fraction of the “interesting” collections. To prevent these GFTR values with small support from dominating the analysis, we apply an adjustment to each GFTR value equal to the fraction of all “interesting” samples (within season) that have nonzero “catch” from the given grid cell.

### 3.5. CRITERIA FOR IDENTIFYING “INTERESTING” SAMPLES

Both the PSCF and the GFTR techniques require that some subset of the samples be designated as significant (or “interesting”) based on the measured content of the collection. A typical approach is to set a criterion value equal to some pre-selected quantile (e.g. the 0.75 quantile) among the measured values for the pollution content across the sample record.

For our seasonal analyses, each season (Spring, Summer, Fall, Winter) is represented by the data aggregated across four years of the SCENES project. In each of these four subsets of the total sample record, we have used criterion values set at the within-season 75<sup>th</sup> percentile. The sample sizes and criterion values for these four groups are shown in Table 1.

**Table 1: Seasonal Criterion Values for Identification of “Interesting” Samples and Corresponding Sample Sizes**

Season	Total # of Samples	Mean PM2.5 ( $\mu\text{g}/\text{m}^3$ )	0.75 Quantile Criterion Value ( $\mu\text{g}/\text{m}^3$ )
Summer	298	3.996	4.725
Fall	310	2.792	3.515
Winter	324	1.603	2.029
Spring	283	3.162	4.039

### 3.6. CONFIDENCE INTERVALS USING BOOTSTRAP

To obtain confidence interval estimates of PSCF, trajectories within each of the four seasons were randomly sampled with replacement using the total number of trajectories as the sample size. The PSCF statistic was calculated for each resampling of back-trajectories. This process was repeated 1000 times, and the 2.5 and 97.5 percentiles of the distribution of PSCF statistics were used to estimate the bounds of 95% confidence intervals.

For each season and potential source, material collection days were sampled with replacement using the total number of collection days as the sample size. The GFTR statistic was calculated, and this process was repeated 1000 times. The 2.5 and 97.5 percentiles of the distribution of GFTR statistics were used to estimate the bounds of 95% confidence intervals.

## 4. RESULTS

### 4.1. PSCF Results

Using the back-trajectories described in Section 3.1 along with the criterion values specified in Table 1 for identifying “interesting” samples, PSCF analysis was performed for each season across the one-degree resolution grid that was depicted earlier in Figure 1. The point-estimates of PSCF for each grid cell through which back trajectories crossed are shown in Figure 3. Meanwhile, the lower bounds of the bootstrap 95% confidence interval for PSCF are pictured in Figure 4.

The source regions suggested by the raw PSCF and the bootstrap lower confidence bound (PSCF-LCB), respectively, in each season are essentially similar. The PSCF-LCB is intended, of course, to highlight grid cells in which we can have greater confidence that the PSCF score is relatively high. [Note: the truncation of the easternmost cells of the grid in the PSCF-LCB charts is due to an inadvertent misspecification of the grid.]

### 4.2. GFTR Results

Using the forward-trajectory framework for hybrid receptor modeling described in 3.4 and the criterion values specified in Table 1, GFTR values were calculated for each cell in the grid. The (point-estimate) GFTR values shown in Figure 5 have been normalized relative to the maximum score within each season.

In Figure 6, we see the lower bounds of 95% confidence intervals on GFTR (GFTR-LCB) obtained with the bootstrap analysis. Again, scores have been normalized relative to the maximum score within each season.

We readily observe that there is comparatively little difference between the GFTR and GFTR-LCB estimates.

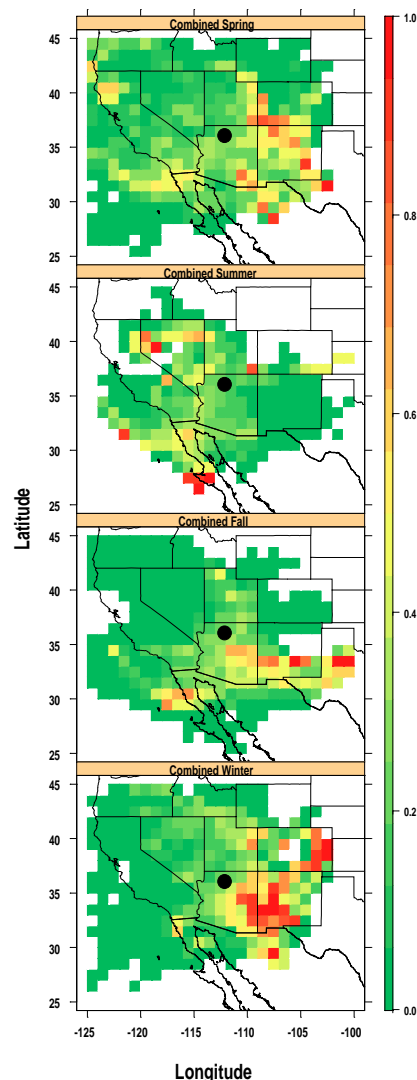


**Figure 3. PSCF analysis by season for potential sources of PM<sub>2.5</sub> in samples collected at Hopi Point, AZ during SCENES.**

This is partly attributable to the adjustments (described earlier in Section 3.4) applied to GFTR values according to the fraction of “interesting” samples to which the hypothetical “source” at that grid point could have contributed fine particulates: The adjustments have already down-weighted the GFTR values associated with broad uncertainty.

## 5. DISCUSSION

We observe that the source regions suggested by GFTR analysis differ somewhat from the corresponding source regions suggested by PSCF analysis. Agree-

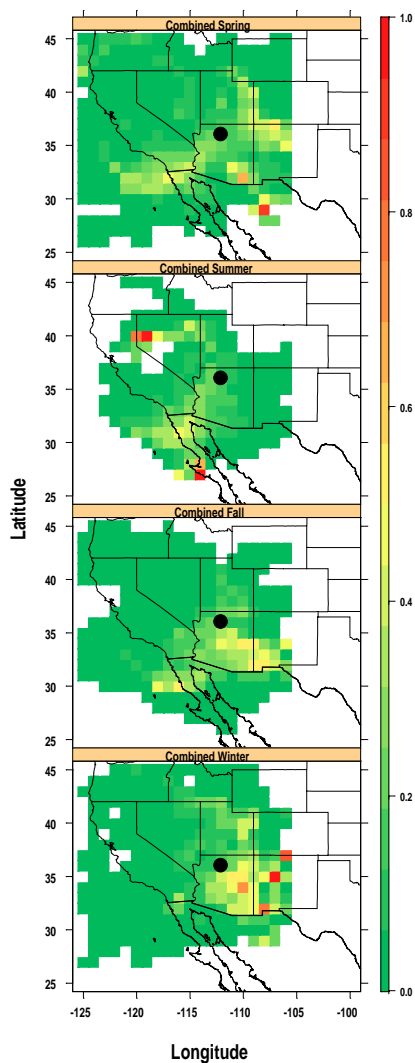


**Figure 4. Lower bounds of 95% confidence intervals on PSCF, by season, for potential sources of PM<sub>2.5</sub> in samples collected at Hopi Point, AZ during SCENES.**

ment between the PSCF and the GFTR source-region estimates appears to be best in the fall with both techniques suggesting sources to the northeast and southeast and, with lesser agreement, both techniques imputing (south-)westward sources. We note that different transport and dispersion models were used in our study for the forward and backward transport descriptors; hence, differences between the results of these two source-location approaches include differences in T&D model skill and cannot be used to argue superiority of one approach over the other.

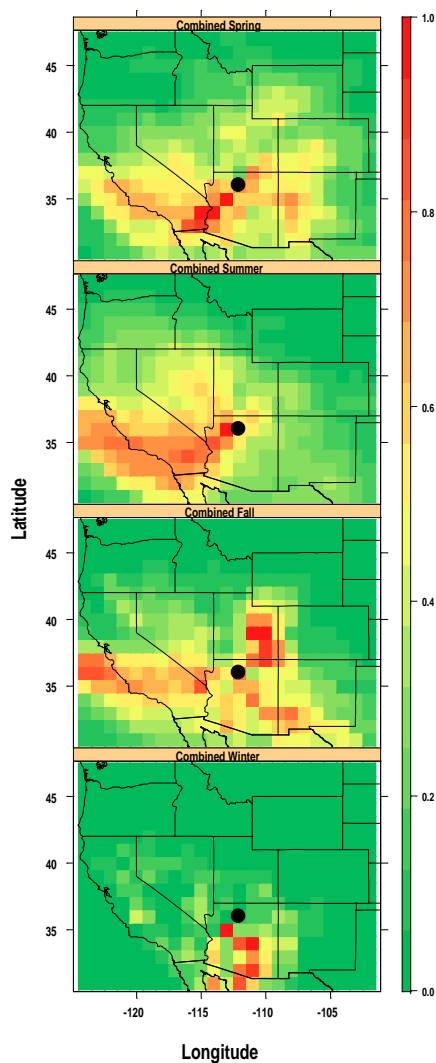


**Figure 5. Gridpoint Forward Transport Ratio (GFTR) analysis by season for potential sources of PM<sub>2.5</sub> in samples collected at Hopi Point, AZ during SCENES. GFTR scores are normalized to the maximum value within season.**

Seasonal variations were clearly evidenced in the results of both techniques. Comparing the grid cells highlighted by our analyses with the major emission sources geo-referenced by Mueller, *et al.* (1986), the GFTR and PSCF graphs show that many different sources probably contributed to samples containing elevated levels of fine particulate matter at the Hopi Point monitor. The facilities listed by Mueller, *et al.* (1986) include numerous smelters and power plants located in Arizona, numerous power plants scattered around California, New Mexico, and Utah as well as smelters in Mex-

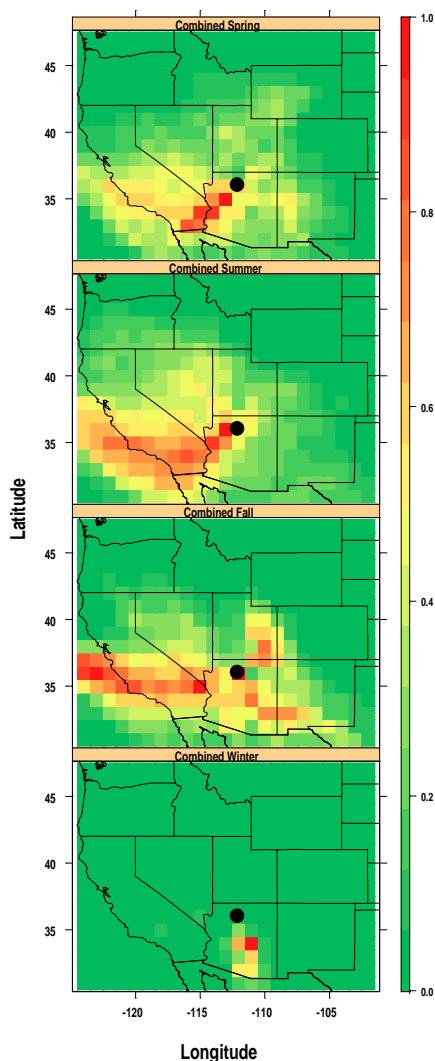


**Figure 6. Lower bounds of 95% confidence intervals on GFTR, by season, for potential sources of PM<sub>2.5</sub> in samples collected at Hopi Point, AZ during SCENES. GFTR scores are normalized to the maximum value within season.**

ico. Their chart does not extend beyond Nevada, Utah and Colorado in the North and also cuts off a portion of New Mexico and almost all of Texas to the East; therefore, we can only speculate as to likely sources corresponding to the high-scoring grid cells from our analysis that lie beyond these states. Major urban areas can obviously be potential sources due to automobile and other emissions.

Comparisons with published results by Vasconcelos (1999) are limited to the spring and fall because those are the only seasonal charts Vasconcelos included in his

paper. The spring chart in Vasconcelos' paper shows the most significant potential sources making a path from western Arizona to Southern California with other significant points scattered around New Mexico, Texas, Utah and Wyoming. The fall chart in Vasconcelos' paper shows a swath of significant potential sources diagonally through Arizona into southern New Mexico, with other scattered points in southern California and Mexico (Vasconcelos, 1999).

Our PSCF results for the fall season shows good general agreement with Vasconcelos (1999) while the GFTR chart for fall shows significant results in Utah along with Arizona, New Mexico and Texas. Utah has a number of coal-fired power plants that may account for high-scoring cells in the GFTR plot. We note that the adjusted GFTR chart, which gives far greater weight to grid cells exhibiting more persistent correlation with the "interesting" samples confines a lot of the significant results in Utah. This may partially explain the particular emphasis that GFTR placed on grid cells corresponding to major urban areas of Southern California owing to the presumed persistence of fine particulate production there.

The PSCF Spring chart puts more significance in New Mexico, Wyoming and Mexico instead of Arizona and Southern California. The GFTR chart also puts more emphasis on the states east of the receptor. We note that the adjusted GFTR agrees very well with Vasconcelos' results (1999).

In his article, Vasconcelos does mention that the winter showed influences from the south and southwest of the receptor site – a finding in essential agreement with our GFTR results.

## 6. SUMMARY

The development of a forward-transport descriptor methodology (namely, GFTR) for hybrid receptor modeling provides complementary methodologies for source location. An inherent advantage to having multiple approaches is that coherency among the estimates enhances confidence in the accuracy of the analysis and enhances the robustness of the capability. Meanwhile, disagreements among these approaches can illuminate latent assumptions in the analysis and provide useful insight.

The forward-transport approach described herein appears to have given results more consistent with benchmark published results. Our forward-transport approach included an adjustment whose effect is to down-weight potential source locations whose possible contributions of effluent are confined to a small fraction of the total number of high-concentration samples. This adjustment consequently assigns relatively higher

weight to grid points that are more consistently imputed as possible sources for high-concentration samples.

The ability to assign a (conditional) probabilistic interpretation to the spatial statistic of either technique (PSCF or GFTR) opens possibilities for defensible assessments of statistical significance and confidence interval estimation.

Numerous ideas for future methodological enhancements have already been contemplated. Those plans include performing studies to obtain a better understanding of for which types of scenarios/contexts each method is best suited.

## 7. REFERENCES

- Ashbaugh, L. L., Malm, W. C. & Sadeh, W. Z. (1985). A residence time probability analysis of sulfur concentrations at Grand Canyon National Park. *Atmospheric Environment*, 19, 1263-1270.
- Begum, B., Kim, E., Jeong, C.-H., Lee, D.-W. & Hopke, P. (2005). Evaluation of the potential source contribution function using the 2002 Quebec forest fire episode. *Atmospheric Environment*, 39, 3719-3724.
- Center for Air Pollution Impact and Trend Analysis, School of Engineering, Washington University, St. Louis (n.d.). *SCENES data*. Retrieved from CAPITA Web site: <http://capita.wustl.edu/CAPITA/DataSets/SCENES/scenes.html>.
- Hopke, P.K., Li, C.L., Ciszek, W., Landsberger, S. (1995). The use of bootstrapping to estimate conditional probability fields for source locations of airborne pollutants. *Chemometrics and Intelligent Laboratory Systems*, 30, 69-79.
- Grell, G., Dudhia, J., & Satuffer, D. (1994). A description of the fifth-generation Penn State/NCAR mesoscale model (MM5). NCAR / TN-398 + STR. Retrieved on 30 September 2005 from <http://www.mmm.ucar.edu/mm5/mm5-home.html>
- Kalnay, E., Kanamitsu, M., & Kistler, R. (1996). The NCEP/NCAR 40-year reanalysis project. *Bulletin of the American Meteorological Society*, 77, 437-471.
- Kienzle, M., & Capuano M. (1989). Software requirements specification for the short-range layered atmospheric model (SLAM) CSCI of the Integrated RPP Evaluation System (IRES). ENSCO, Inc. (Melbourne, Florida) Technical Report.
- Malm, W. C., Johnson, C. E., & Bresch, J. F. (1986). Application of principal component analysis for purposes of identifying source-receptor relationships in receptor methods for source apportionment. In Pace, T. G. (ed.), *Air Pollution Control Association. Pittsburgh, PA*, pp. 127-148.
- Mueller, P. K., Hansen, D. A., & Watson, Jr., J. G. (1986). The Subregional Cooperative Electric Utility, Department of Defense, National Park Service, and EPA Study (SCENES) on Visibility: An Overview. Report EA-4664-SR, Electric Power Research Institute, Palo Alto, CA.
- National Weather Service Phoenix AZ Weather Forecast Office, (n.d.). *The Arizona Monsoon*. Retrieved from National Weather Service - NWS Phoenix Web site: <http://www.wrh.noaa.gov/psr/general/monsoon/>.
- Pielke, R. A., Cotton, W. R. Walko, R. L., Tremback, C. J., Lyons, W. A., Grasso, L. D., Nicholls, M. E., Moran, M. D., Wesley, D. A., Lee, T.J. & Copeland, J.H. (1992). A comprehensive meteorological modeling system – RAMS. *Meteorology and Atmospheric Physics*, 49, 69-91.
- Vasconcelos, L. A., Macias, E. S., & White, W. H. (1994). Aerosol composition as a function of haze and humidity levels in the southwestern U.S. *Atmospheric Environment*, 28(22), 3679-3691.
- Vasconcelos, L. A., Kahl, J. D., Liu, D., Macias, E. S., & White W. H. (1996). A tracer calibration of back trajectory analysis at the Grand Canyon. *Journal of Geophysical Research*, 101(D14), 19329-19335.
- Vasconcelos, L.A. (1999). Seasonal transport of fine particle to the Grand Canyon. *Journal of the Air & Waste Management Association*, 49, 268-278.